04,08

Wide-band EPR spectroscopy of a $Lu_3Al_5O_{12}$:Tb^{3+} crystal

© G.R. Asatryan[1], G.S. Shakurov[2], K.L. Hovhannesyan[3], A.G. Petrosyan[3]

[1] Ioffe Institute,
St. Petersburg, Russia
[2] Zavoisky Physical-Technical Institute, FRC Kazan Scientific Center of RAS,
Kazan, Russia
[3] Institute for Physical Research, National Academy of Sciences of Armenia,
Ashtarak-2, Armenia

E-mail: hike.asatryan@mail.ioffe.ru

Received December 16, 2022
Revised December 16, 2022
Accepted December 22, 2022

In a single crystal of lutetium aluminum garnet ($Lu_3Al_5O_{12}$, LuAG) in the frequency range of 37−210 GHz, at a temperature of 4.2 K, the EPR spectra of non-Kramers Tb^{3+} impurity ions were recorded. The measurement results indicate that Tb^{3+} ions replace Y^{3+} ions in the dodecahedral position with local D_2 symmetry. The value of the g factor, the hyperfine structure constant, and the energy interval between the ground and the first excited nondegenerate sublevels of the ground multiplet are determined. Weak satellite signals were also registered, the origin of which is associated with the formation of antisite defects in the environment of paramagnetic Tb^{3+} centers.

Keywords: hyperfine interaction, rare earth ions, spin Hamiltonian, non-Kramers ion.

DOI: 10.21883/PSS.2023.03.55581.554

1. Introduction

Lutetium aluminum garnet $Lu_3Al_5O_{12}$ (LuAG) activated by a number of rare-earth ions is a laser crystal, scintillator and phosphor with a variety of technological applications. Along with a wide transparency region and high stability, it is denser and harder than the widely used structural analogue — yttrium aluminum garnet ($Y_3Al_5O_{12}$; YAG). The exceptional fluorescent properties of the Tb^{3+} ion with a large set of lines in the visible region of the spectrum provide a bright glow of phosphors with this ion in the lemon-yellow zone, which have found applications in devices based on cathode ray tubes and projection screens [1]. High-efficiency phosphors have been created, including those based on LuAG:Tb [2]. In the YAG:Ce, Tb [3] and LuAG:Ce, Tb [4] garnets, the functional role of the Tb^{3+} ion is in energy transfer $Tb^{3+} \rightarrow Ce^{3+}$. The capture of electrons at defects in the crystal lattice was considered in the work [4] among the factors hindering the increase in the light yield of LuAG:Ce,Tb.

With appearing of blue semiconductor pump sources for direct excitation of the upper $^5D_4$ laser level on fluoride crystals, efficient lasing was obtained on the green and yellow lines of the Tb^{3+} ion [5,6]. Yellow laser light is very relevant for the treatment of skin and eyes. To date, laser generation of Tb^{3+} ions has not been obtained in oxide crystals. The reasons remain not completely clear, pointing to the need for further spectroscopic analysis. Defects in the crystal lattice can also play a certain role, since the thermal load on the crystal can increase when lasing is excited in the presence of even minor defects in the lattice, including violations or stresses.

The method of electron paramagnetic resonance (EPR) is one of the direct methods for studying the spectroscopic properties of materials. In our recent publications [7,8] we reported on the EPR observation in YAG crystals at frequencies of 94 and 130 GHz of both the main Tb^{3+} centers and the Tb^{3+} in the nearest environment of which there are unusual (nonequivalent) substitutions by Y^{3+} ions of Al^{3+} ions at octahedral sites (a-sites), or substitutions by Al^{3+} ions Y^{3+} ions at c-sites.

For the first time the present work discovered and studied the terbium impurity centers in a LuAG crystal in detail by broadband EPR spectroscopy, and information was obtained on the energy interval between the ground and the first excited nondegenerate sublevels of the ground multiplet of the Tb^{3+} ion.

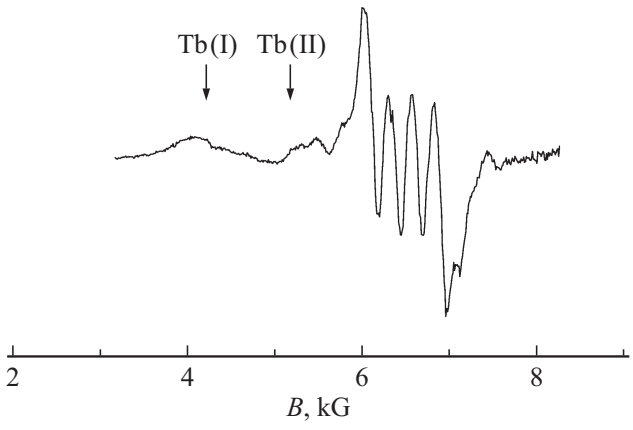

Figure 1. EPR spectrum of Tb^{3+} ion in lutetium aluminum garnet at $T = 4.2$ K, $B \parallel \langle 100 \rangle$ and frequency 175 GHz.

2. Experimental results

The LuAG:Tb^{3+} (0.15 at.%) crystal was produced in the Institute for Physical Research of the National Academy of Sciences of the Republic of Armenia (Ashtarak-2, Armenia). Crystal growth was carried out by the modified Bridgman method [9,10] using high-purity oxides (Lu_2O_3, Al_2O_3, Tb_2O_3), molybdenum containers and seed crystals oriented along the $\langle 001 \rangle$ axis at a growth rate of 1.5 mm/h. Garnet LuAG has a region of homogeneity and can be described as a solid solution $Lu_3[Al_{2-x}Lu_x]Al_3O_{12}$ $(0.01 \leq x \leq 0.05)$ [11] (see also the phase diagram of the $Lu_2O_3-Al_2O_3$ [12]), therefore, to compensate for the occupation of octahedral sites by lutetium ions and avoid precipitation of secondary phases, the initial melt composition contained a small excess (0.5 at.%) of Lu_2O_3 oxide. The crystal obtained under the conditions used was free from secondary phases and light-scattering inclusions. With $\langle 001 \rangle$ orientation, facets forms of the growth are displaced to a crystal periphery and a major part of the crystal bulk has no such flaws. The studies were prepared with providing a sample made of central crystal areas, which are free of facets sized as $8 \times 8 \times 6\,mm^3$, which was oriented on the X-ray diffractometer. Based on the size factors, the Tb^{3+} ($R_{Tb} = 1.04$ Å) ions should replace the Lu_{3+} ($R_{Lu} = 0.977$ Å) dodecahedral positions in the LuAG lattice with an octal oxygen environment.

The EPR spectra of Tb^{3+} ions were recorded on a broadband EPR spectrometer built at the Kazan Physical-Technical Institute [13] in the frequency range 37–210 GHz. Several different paramagnetic centers have been found. The most intense lines belonged to terbium ions localized in dodecahedral positions. The Fig. 1 shows the EPR spectrum shape obtained at the frequency of 175 GHz in the orientation of the $B \parallel \langle 100 \rangle$.

Although the hyperfine structure (HFS) is not completely resolved, the presence of four lines (^{159}Tb, $I = 3/2$, natural abundance 100%) clearly indicates that the spectrum belongs to the Tb^{3+} ion. The localization of terbium in the dodecahedron is confirmed by the characteristic angular dependence of the EPR spectra measured at a frequency of 150 GHz and shown in Fig. 2. The crystal was rotated in the (110) plane. In this case, for simplicity, the figure shows only the position of the low-field HFS component in the magnetic field.

Most of the rare earth elements enter lutetium-aluminum garnet in the dodecahedral c-position, replacing Lu^{3+} in the crystal lattice. There are six such positions in LuAG crystals; therefore, six EPR lines of magnetically nonequivalent centers can be observed for an arbitrary orientation of the crystal. As was found earlier, the situation is simplified for Tb^{3+} ions, since for them $g_\perp = 0$, and for an arbitrary orientation of the crystal, only three magnetically nonequivalent terbium centers with axial symmetry along the $\langle 001 \rangle$ axis are observed. When the crystal rotates in the (100) plane, only two of the three magnetically nonequivalent centers are observed. Moreover, the direction of the maximum g-factor coincides with the crystallographic direction $\langle 100 \rangle$.

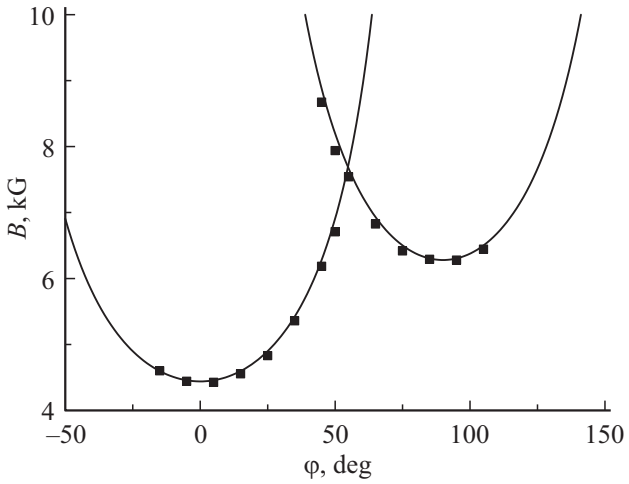

Figure 2. Orientation dependences of the EPR spectra measured at a frequency of 150 GHz and $T = 4.2$ K. Rotation in the (110) plane, the angle $\varphi = 0^0$ corresponds to the direction $B \parallel \langle 100 \rangle$. The dots — the experiment, the lines — the calculation.

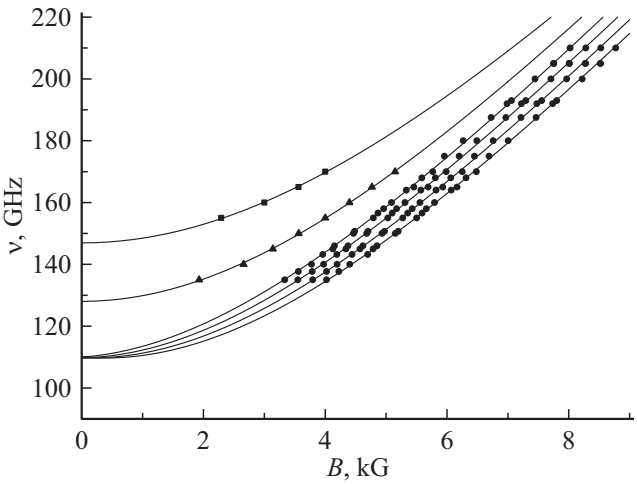

Figure 3. Field-frequency dependences of the EPR spectra of the Tb^{3+} ion in the $Lu_3Al_5O_{12}$ crystal, for the $B \parallel \langle 001 \rangle$ orientation. Points — center Tb^{3+}, squares — center Tb^{3+}(I), triangles — center Tb^{3+}(II), lines — calculation.

The obtained angular dependence for LuAG agrees with the results for the YAG crystal. Measurement of the EPR spectra at different frequencies allowed to plot the field-frequency dependence of the spectra, which is shown in Fig. 3. Due to incompletely resolved HFS, the position of the lines in the magnetic field was determined from the absorption spectra obtained after integrating the EPR spectra. It follows from this dependence that the observed EPR spectra are due to resonant transitions between two singlet electronic states, which form a quasi-doublet with splitting in a zero magnetic field (ZFS). The experimental results obtained have much in common with the results of studies of YAG:Tb crystals. However, in addition to the differences in the values of the spectroscopic parameters, there is a noticeable difference in the widths of the EPR

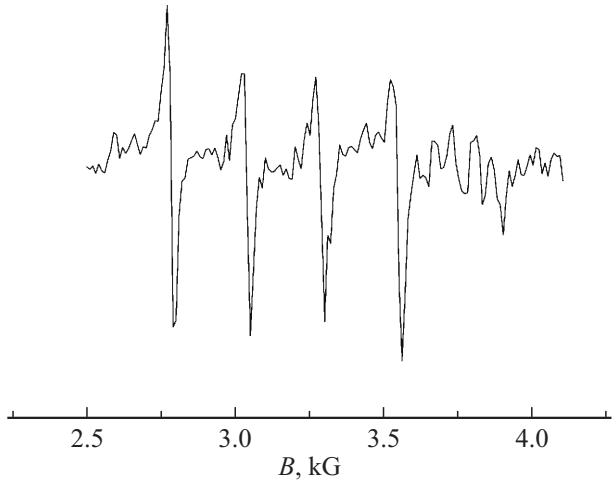

Figure 4. EPR spectrum of $Lu_3Al_5O_{12}$:Tb crystal at 77.7 GHz at temperature $T = 4.2$ K and an arbitrary orientation of the magnetic field.

lines. At the same impurity concentration, the lines of terbium in lutetium-aluminum garnet are ~ 3 times wider than the lines in yttrium-aluminum garnet.

In addition to the intense center Tb^{3+}, several centers with lower intensity and close spectroscopic parameters were detected. Only two of them were studied, the centers designated as Tb^{3+}(I) and Tb^{3+}(II) in Fig. 1 gave weak satellite lines in magnetic fields smaller than for the main center (Fig. 1). The Tb^{3+}(I) and Tb^{3+}(II) centers, like the main center, had broad EPR lines, and we failed to resolve their HFS in the magnetic fields available to us. We were only able to estimate the g-factors and ZFS values of the centers of gravity of these lines. Note that the superposition of satellite lines on the main spectrum increased the error in determining the position of the lines (see Fig. 3) and, accordingly, affected the accuracy of determining the spectroscopic parameters.

We also detected weak EPR signals from a low-symmetry terbium center, the nature of which is still unclear. The well-resolved hyperfine structure indicates that the center belongs to terbium. Figure 4 shows the EPR spectrum at a frequency of 77.7 GHz for an arbitrary orientation of the crystal. The lines of this center are substantially narrower than the lines of the main center of terbium, and the direction of the principal axes of the g-tensor does not coincide with the main crystallographic directions. A detailed description of this center will be made in a separate work.

To find the spectroscopic parameters of the paramagnetic center of dodecahedral symmetry, we used the spin Hamiltonian [14] with effective spin $S = 1/2$ and nuclear spin $I = 3/2$. The ZFS value is denoted by the symbol Δ.

$$H = \mu_B S \cdot g \cdot B + (\Delta_x S_x + \Delta_y S_y) + A S_z I_z, \qquad (1)$$

where, μ_B — Bohr magneton, $S = 1/2$ — effective electron spin. The first term in (1) describes the Zeeman interaction,

Parameters of Tb^{3+} centers in the $Lu_3Al_5O_{12}$ crystal

Center	g_z	A_z (GHz)	Δ (GHz)
Tb^{3+}	15.27	5.16	109.7
Tb^{3+} (I)	15.17		146.96
Tb^{3+} (II)	15.56		128.04

the second — the splitting of electronic levels in a zero magnetic field $\Delta = (\Delta_x^2 + \Delta_y^2)^{1/2}$, and the latter is a hyperfine interaction with a constant A.

Using analytical expressions for energy levels and experimental data (Fig. 3), we determined the values of spectroscopic parameters — g-factors and Δ for terbium centers in LuAG. The results are shown in the Table.

3. Discussion

Based on the pronounced hyperfine structure (four HFS components) and the angular dependences, the observed signals in $Lu_3Al_5O_{12}$:Tb are uniquely assigned to Tb^{3+} ions occupying dodecahedral positions of the garnet crystal lattice (symmetry D_2) replacing the Lu^{3+} ion. The ground state of the non-Kramers ion Tb^{3+} (electronic configuration $4f^8$, $^7F_6$ $(L = 3,\ S = 3,\ J = 6)$) in a crystal field of axial symmetry splits into six doublets characterized by $M_J = \pm 6, \pm 5, \ldots, \pm 1$ and to a singlet with $M_J = 0$ [14]. The lowest state is the $M_J = \pm 6$ doublet. The effect of admixture of excited states by the crystal field causes the splitting of this doublet in zero magnetic field and leads to a decrease in the value of $g_{\|}$ relative to its value for the pure state $M_J = \pm 6$, which is 18.

Low-intensity satellite signals observed in the EPR spectra of the $Lu_3Al_5O_{12}$:Tb single crystal also belong to Tb^{3+} ions localized at c-sites, but the nearest environment of such centers is distorted by the presence of a defect. Since the substitution is isovalent, it is obvious that these defects cannot be associated with local charge compensation. In LuAG single crystals, such disturbances can be unusual (nonequivalent) substitutions of Lu^{3+} ions for Al^{3+} ions at octahedral sites (a-sites), or substitutions of Al $^{3+}$ Lu^{3+} ions at c-nodes. Antisite defects are not paramagnetic and cannot be directly detected by the EPR method. However, due to a significant difference in ionic radii ($R^{3+}_{Al\,(6)} = 0.53$ Å, $R^{3+}_{Lu\,(8)} = 0.977$ Å, $R^{3+}_{Lu\,(6)} = 0.861$ Å), such substitutions lead to a change in interatomic distances and, accordingly, to a significant deformation of the crystal lattice near the paramagnetic center. As a result, oxygen ions will be displaced, which are simultaneously part of both the immediate environment of Tb^{3+} and the distorted site (Lu^{3+} or Al^{3+}). This leads to the formation of unequal crystal fields for those Tb^{3+} ions whose cationic environment contains AD.

Attention is drawn to the observed significant difference in the widths of the EPR lines of terbium in crystals of lutetium-aluminum and yttrium-aluminum garnet, which are

similar in structure, almost by a factor of 3. The difference in the widths of the EPR lines of the Mo^{3+} ion in LuAG, in comparison to YAG was observed earlier in the paper [15].

4. Conclusion

The method of the wideband EPR spectroscopy has allowed finding and studying the Tb^{3+} non-Kramers ions in the lutetium aluminum garnet, which substitute the Y^{3+} ions in the dodecahedral position of the crystal lattice. The g-factor 15.27, the hyperfine structure constant 5.16 GHz, and the energy interval $\Delta = 109.7$ GHz between the main and the next excited multiplet of the rare-earth ion Tb^{3+} are determined. The low-intensity EPR lines of the Tb^{3+} ion are due to centers in the immediate surroundings of which an anti-site defect is localized with Al^{3+} sites being replaced by Lu^{3+} ions.

Acknowledgments

The authors are grateful to N.G. Romanov for his interest in the work and a detailed discussion of the results, and to V.A. Shustov for crystal orientation on the X-ray diffractometer.

Funding

The study was financially supported by the Russian Foundation for Basic Research (the RFBR grant No. 20-52-05002 Arm_a) and the Science State Committee of the Republic of Armenia (the grant 20RF-024).

The study was carried out in the Zavoisky Physical-Technical Institute, FRC Kazan Scientific Center of RAS under the Government Assignment.

Conflict of interest

The authors declare that they have no conflict of interest.

References

[1] I. Kandarakis, D. Cavouras, G.S. Panayiotakis, C.D. Nomicos. Phys. Med. Biol. **42**, 1351 (1997).
[2] Y. Liao, D. Jiang, T. Feng, J. Shi. J. Mater. Res. **20**, *11*, 2934 (2005).
[3] V. Khanin, A.-M. van Dongen, D. Buettner, C. Ronda, P. Rodnyi. ECS J. Solid State Sci. Technology **4**, *8*, R128 (2015).
[4] J. M. Ogiegło, A. Zych, K.V. Ivanovskikh, T. Jüstel, C.R. Ronda, A. Meijerink. J. Phys. Chem. A **116**, *33*, 8464 (2012).
[5] C. Krankel, D.T. Marzahl, F. Moglia, G. Huber, P. Metz, Las. Photon. Rev. **10**, 548 (2016).
[6] S. Kalusniak, E. Castellano-Hernández, H. Yalçinoğlu, H. Tanaka, C. Kränkel. Appl. Phys. B **128**, 33 (2022).
[7] E.V. Edinach, Y.A. Uspenskaya, A.S. Gurin, R.A. Babunts, H.R. Asatryan, N.G. Romanov, A.G. Badalyan, P.G. Baranov. Phys. Rev. B **100**, 104435 (2019).
[8] G.R. Asatryan, E.V. Edinach, Yu.A. Uspenskaya, R.A. Babunts, A.G. Badalyan, N.G. Romanov, A.G. Petrosyan, P.G. Baranov. FTT **62**, *11*, 1875 (2020). (in Russian).
[9] Kh.S. Bagdasarov. Kristallizatsiya iz rasplava. In: Sovremennaya kristallografiya / Pod red. B.K. Vaynshtein. Nauka, M. (1980). T. 3. P. 337. (in Russian).
[10] A.G. Petrosyan. J. Crystal Growth **139**, 372 (1994).
[11] A.G. Petrosyan, G.O. Shirinyan. Neorgan. materialy **29**, *2*, 258 (1993). (in Russian).
[12] A.G. Petrosyan, V.F. Popova, V.V. Gusarov, G.O. Shirinyan, C. Pedrini, P. Lecoq. J. Crystal Growth **293**, 74 (2006).
[13] V.F. Tarasov, G.S. Shakurov. Appl. Magn. Res. **2**, *3*, 571 (1991).
[14] A. Abragam, B. Blini. Elektronnyj paramagnitnyj rezonans perekhodnykh ionov. Mir, M. (1972). (in Russian).
[15] E.G. Sharoyan, O.S. Torosyan, A.G. Petrosyan, E.A. Markosyan. Izv. AN ASSR. Fizika **12**, 62 (1977). (in Russian).

Translated by E.Potapova